JOURNAL OF MATERIALS SCIENCE 33 (1998) 4015–4020

The effect of Ag additions on the microstructure of aluminium–lithium alloys

N. BOUKOS, E. FLOUDA, C. PAPASTAIKOUDIS
Institute of Materials Science, National Centre for Scientific Research "Demokritos", GR 15310 Agia Paraskevi, Attiki, POB 60228, Greece
E-mail: nboukos@ims.ariadne-t.gr.

Minor quantities of Ag have been added to Al–Li–Cu–Mg–Zr alloys. Their microstructure has been studied by means of optical metallography, transmission electron microscopy and X-ray diffraction. In the high Li, low Cu : Mg ratio alloys the main phases found were δ′, β′, S' and T_1, while fewer T_2 and Al_7Cu_2Fe precipitates were also observed. The addition of up to 0.5 wt % Ag diminishes the δ′ and T_1 precipitates size. This is attributed to a small increase of Li solubility in the matrix. In the low Li, high Cu : Mg ratio alloy the addition of 0.2 wt % Ag resulted in the precipitation of Ω phase simultaneously with δ′, β′, S' and T_1 phases. Due to the low Li concentration an unusual growth of the δ′/β′ precipitates at the expense of the δ′ precipitates was also observed. © *1998 Kluwer Academic Publishers*

1. Introduction

Due to the combination of high mechanical strength and low density aluminium–lithium based alloys have been extensively studied in the past twenty years, in order to replace conventional aluminium alloys in aviation engineering [1, 2]. When the concentration of Li exceeds approximately 1.4 wt % the metastable δ′ phase (Al_3Li), which has an ordered f c c $L1_2$ structure, forms during ageing [3]. This is the major strengthening phase in aluminium–lithium alloys, however due to coplanar slip and strain localization associated with the coherent δ′ precipitates the formation of other phases is desirable.

In 8090 type alloys the other main phases that can grow are the S' (Al_2CuMg), T_1 (Al_2CuLi) and β′ (Al_3Zr) [4, 5]. These phases improve the specific strength up to 100 °C. At higher temperatures the small precipitates of these phases coarsen rapidly and as a result a decline of the mechanical properties is observed. Recent studies [6–9] have revealed that, when in the appropriate phase field, microadditions of silver in alloys containing copper and magnesium, results in the precipitation of the Ω phase, which is stable up to higher temperatures and also further enhances the room temperature mechanical strength of the alloys. The purpose of the present study is to examine the possibility of Ω phase precipitation in Al–Li–Cu–Mg–Zr alloys when minor quantities of Ag are added. In addition the modifications, introduced by the Ag additions, to the microstructure of the alloys are studied.

2. Experimental procedure

The alloys were provided in plate form by the Defence Research Agency (Structural Materials Centre, Farnborough, UK). They were aged in silicone oil in order to minimize the Li losses. The ageing temperature was controlled within ± 1 °C. The nominal chemical composition and the codes of the alloys as well as the ageing conditions are presented in Table I. The ageing temperature and time correspond to peak- and under-aged condition of the alloys, as determined by hardness measurements [10]. The alloys were mechanically polished to a thickness of about 100 μm. The samples used for optical metallography were etched with Kellers reagent in order to enhance grain contrast and subsequently examined under polarised light with a Vickers M17 Metallurgical Microscope. The 3 mm disks used for transmission electron microscopy (TEM) observations were electrolytically polished by a twin jet apparatus at − 40 °C, using a solution of 10% perchloric acid in methanol as the electrolyte. The thin foils were examined under a Philips CM20 TEM operating at 200 kV. All TEM observations were carried out in specimen areas with approximately the same thickness, as judged by the method proposed by Kelly *et al.* [11]. Consequently qualitative estimations of the volume fraction of the precipitates could be made, even though no quantitative measurements of their volume fraction were performed. The X-ray diffraction (XRD) measurements were performed on polished polycrystalline foils with a Siemens D500 powder diffractometer with a graphite secondary monochromator.

3. Results and discussion

Examination of the alloys under the optical microscope revealed that they all exhibited a typical unrecrystallised grain structure with pan-cake shaped grains elongated in the rolling direction. A typical grain structure is shown in the photograph of Fig. 1.

TABLE I Chemical composition of the alloys, heat treatments used and δ′-δ′/β′ precipitates mean diameter

Alloy	A		B		C		D	
Concentration (wt %)	2.4Li:0.7 Mg :1.3Cu:0.12 Zr		2.4Li:0.7 Mg : 1.3Cu:0.12 Zr : 0.2 Ag		2.4Li:0.7 Mg : 1.3Cu:0.12 Zr : 0.5 Ag		1.5Li:0.5 Mg : 2.5Cu:0.12 Zr : 0.2 Ag	
Heat treatment (°C)	170	170	190	190	170	170	170	170
Phase	Size (nm)							
Al_3Li	41	38	37	32	30	29	?	18
Al_3Li/Al_3Zr	62	71	73	61	57	65	?	90

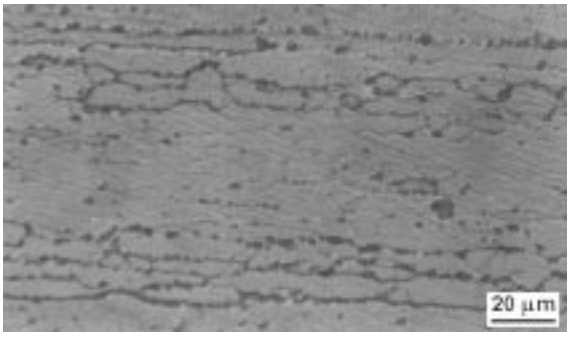

Figure 1 Typical microstructure of alloy C.

TABLE II Phases detected in the studied alloys

Alloy	A		B		C		D	
Heat treatment (°C)	170	170	190	190	170	170	170	170
duration (h)	96	48	48	24	96	48	72	36
Phases								
δ′	+	+	+	+	+	+	+	+
S'	+	+	+	+	+	+	+	+
T_1	+	+	+	+	+	+	+	+
T_2	+	+	+	+	+	+	−	−
Ω	−	−	−	−	−	−	+	+
Al_7Cu_2Fe	+	+	+	+	+	+	−	−

Table II summarises the phases detected in all the alloys examined, for comparison reasons.

First the results concerning alloys A, B and C will be presented as the only difference between them is the Ag concentration ranging from 0–0.5 wt %. The major precipitating phase in these alloys is δ′. A homogeneous distribution of δ′ precipitates was observed in both under- and peak-aged condition. Fig. 2 is a typical dark field micrograph of δ′ precipitates obtained with a (1 0 0) superlattice spot. The precipitates have an almost spherical morphology. They nucleate either homogeneously in the matrix or heterogeneously on Al_3Zr precipitates which are isostructural to them. The latter results in composite δ′/β′ precipitates that have been observed in previous studies [12, 13]. The mean diameter of δ′ and δ′/β′ precipitates is presented in Table I, where the established bimodal size distribution of δ′ and δ′/β′ precipitates [14] is obvious. These results are obtained from the measurements of the size of 200 δ′ precipitates in two different locations per sample, from each of the two samples examined per heat treatment. It can be noticed that the size of the δ′ precipitates tends to decrease as the Ag content increases. This observation may suggest that the addition of Ag slightly increases the solubility of Li in the matrix and thus lowers the fraction of precipitating Li. Baumann and Williams [15] reported that the addition of Ag lowers the δ′ solvus and consequently decreases the solubility of Li in the matrix. They studied a ternary Al–1.8Li–1Ag alloy. The conflict between their results and the present study may be attributed to the following reasons. The Ag concentration in the present investigation varies between 0.2–0.5 wt %. This concentration range

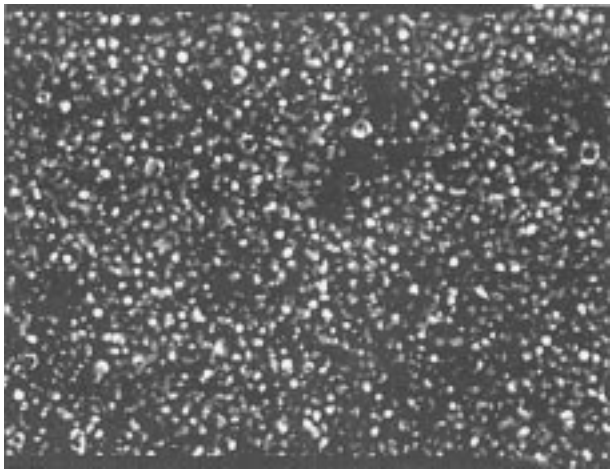

Figure 2 DF micrograph of homogeneously distributed δ′ precipitates of B alloy in under-aged condition. Magnification × 38 000.

might represent a transitional region where the Li solubility in the matrix increases, while at higher Ag concentrations the solubility diminishes. Another important reason is that the present alloys are complex AlLiCuMgZrAg alloys, compared to the simpler ternary AlLiAg alloy studied by Baumann and Williams. Consequently, more complicated mechanisms and interactions, not yet fully understood, are likely to take place. The high binding energy between zirconium and vacancies could be a mechanism of that kind. A study of an AlLiCuMgZrAg alloy with 1 wt % Ag could possibly resolve the above discrepancy.

As can be seen in the dark field image of Fig. 3a, inside the grains there are regions depleted of δ′ precipitates. Fig. 3b is a bright field micrograph of the same area. The relatively large precipitates that correspond to the δ′ depleted region is of the quasicrystalline T_2 phase (Al_6CuLi_3). This phase is icosahedral, exhibiting a $m\bar{3}\bar{5}$ point symmetry [16, 17] and grows by a solid state reaction usually at grain boundaries and rarely inside the grains [18]. The characteristic five-fold symmetry axis of the T_2 phase is evident in the convergent beam electron diffraction pattern of Fig. 3c. When the T_2 precipitates grow inside the grains they are surrounded by an intense strain field and a δ′ precipitate free region, as can be noticed in Fig. 3(a and b). T_2 precipitates were also observed to grow at high angle grain boundaries. Fewer Al_7Cu_2Fe precipitates were also detected at grain boundaries. This phase precipitates due to iron impurities that prexist in the aluminium used for the preparation of the alloys. It must be noticed that no equilibrium δ precipitates (AlLi) were found either at grain boundaries or inside the grains.

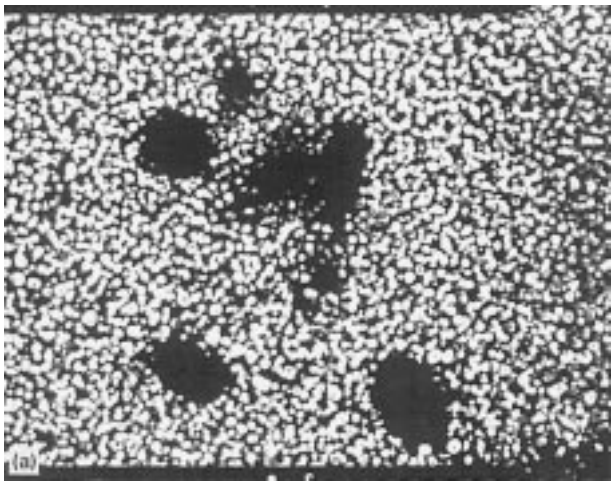

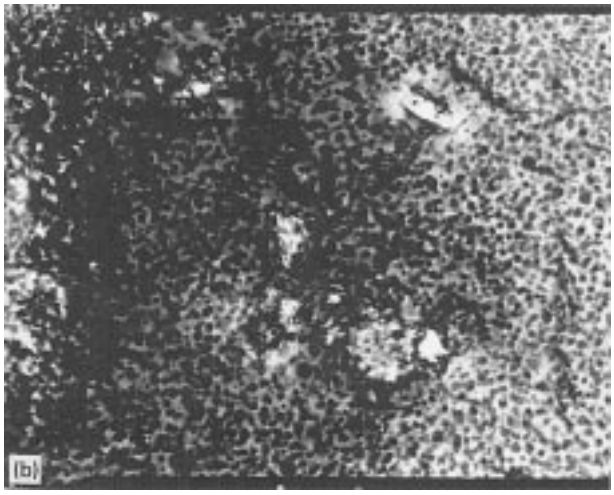

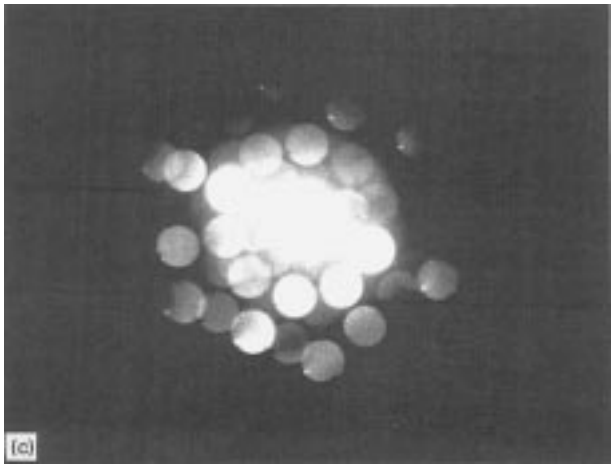

Figure 3(a) DF micrograph of δ′ precipitates of A alloy in under-aged condition. Magnification × 2000; (b) BF micrograph of the same area showing T_2 precipitates grown inside a grain. Magnification × 20 000; (c) CBED pattern exhibiting five fold symmetry axis of a T_2 precipitate.

Apart from δ′ the other major strengthening phase detected was S'. It has an orthorhombic structure with $a = 0.405$ nm, $b = 0.905$ nm, $c = 0.724$ nm and grows as rods along $\langle 1\,0\,0 \rangle$ matrix directions or forms laths with $\{210\}$ habit planes [19]. It was found to nucleate either homogeneously inside the grains or heterogeneously at subgrain boundaries, Fig. 4. In the bright field micrograph of Fig. 5a the two morphologies of S' precipitates can be distinguished. The associated selected area diffraction pattern is presented in Fig. 5b. The zone axis is [0 0 1] and the S' spots can be seen near the δ′ superlattice spots. Taking into account that S' rods grow along $\langle 1\,0\,0 \rangle$ matrix directions the fine disks seen in Fig. 5a correspond to the diameter projection, in the foil plane, of S' rod shaped precipitates grown along the [0 0 1] matrix direction. The S' rods grown along [1 0 0] and [0 1 0] matrix directions intersect each other at right angles. Increasing the ageing time results in a significant increase of the S' precipitates size, whilst the addition of Ag does not affect their size or distribution. As can be noticed from Figs 4 and 5a the primary morphology of the S' precipitates is that of rods. This is in agreement with the observations of Gupta *et al.* [19] for a ternary AlCuMg alloy with a similar composition. Whether or not the S' rods coalesce and form laths depends on the density of nucleation sites and on the extent of growth of the S' rods [19–21]. In the present study the degree

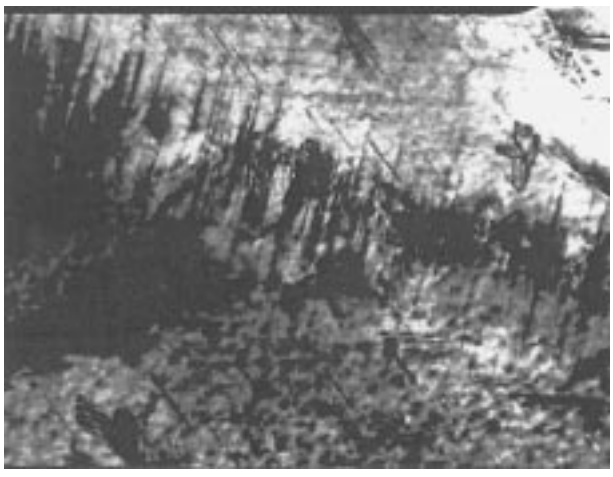

Figure 4 BF of S' precipitates grown either homogeneously inside a grain or heterogeneously on a subgrain boundary. Magnification × 38 000.

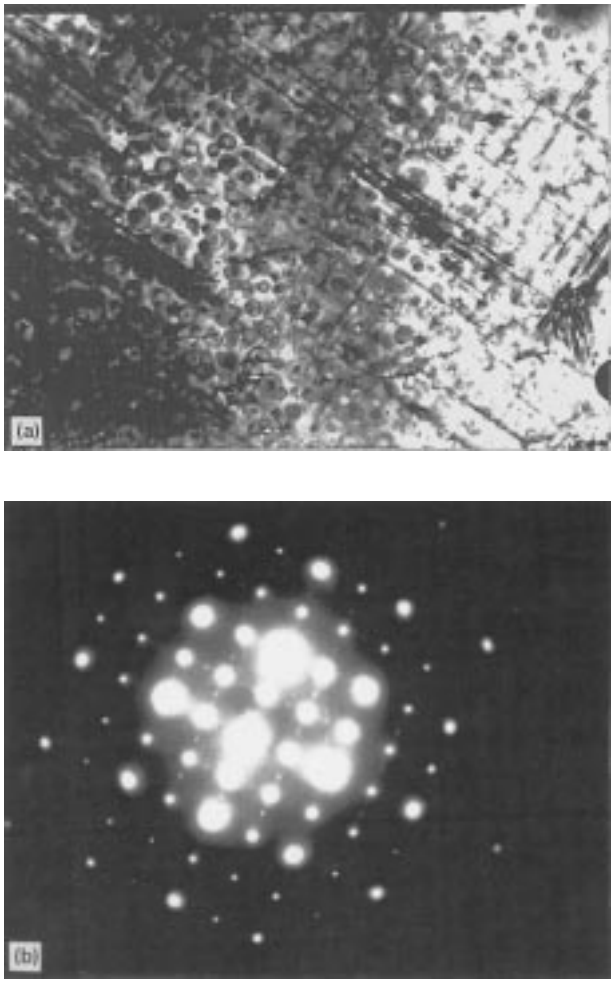

Figure 5(a) BF micrograph of S' rods grown along three $\langle 1\,0\,0 \rangle$ matrix directions. Magnification × 38000; (b) associated SAD pattern indicating [0 0 1] zone axis.

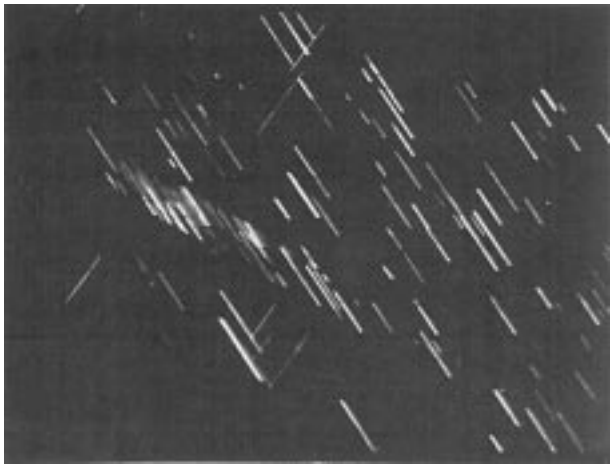

Figure 6 Typical DF micrograph of S' precipitates. Magnification × 38 000.

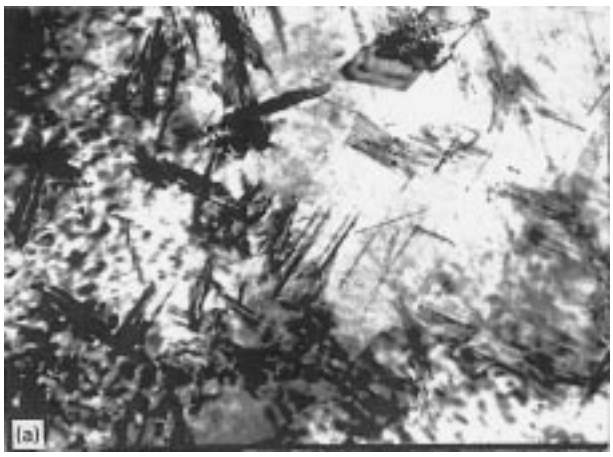

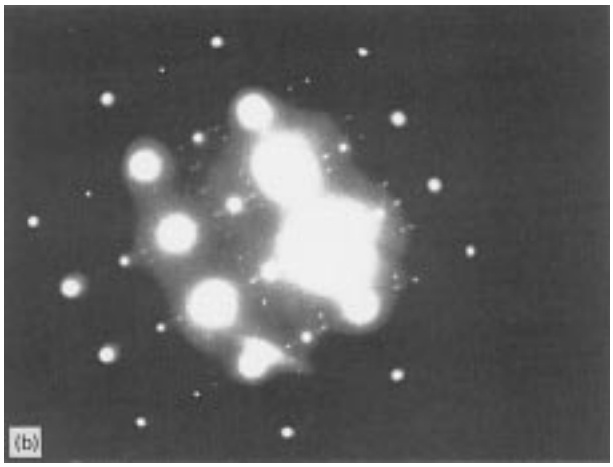

Figure 7(a) BF micrograph of edge-on T1 plates. Also shown are S' precipitates. Magnification × 38 000; (b) associated SAD pattern indicating $[\bar{1}\,1\,2]$ zone axis.

of supersaturation, that depends on total amount of Cu and Mg, is relatively low. Also the ageing time for the given temperature is short, i.e., no over-ageing occurs. Consequently the coalescence of the S' rods is not favoured in the interior of the grains. S' laths were observed to form mainly at subgrain boundaries. This can be attributed to the high density of dislocations that act as nucleation sites for S' precipitates, which coalesce and form laths during ageing. A typical dark field micrograph of S' precipitates along $[5\,1\,2]$ and $[1\,5\,\bar{2}]$ matrix directions, obtained with a $[\bar{1}\,1\,2]$ zone axis orientation, is presented in Fig. 6.

The third strengthening phase detected is T_1. It is hexagonal with $a = 0.497$ nm, $c = 0.935$ nm and precipitates as thin plates on $\{1\,1\,1\}$ matrix planes [22, 23]. Fig. 7a shows a typical distribution of edge-on T_1 precipitates. The volume fraction of these precipitates is significally lower than that of the S' precipitates. The zone axis is $[\bar{1}\,1\,2]$ as can be verified from the selected area diffraction pattern of Fig. 7b. The T_1 spots are seen parallel to $\{1\,1\,1\}$ matrix spots. The streaks along $[0\,\bar{2}\,1]$, $[2\,0\,1]$ and $[\bar{1}\,1\,0]$ are due to S' rods and a comparison of their intensity indicate nearly equal S' populations along the three $\langle 1\,0\,0 \rangle$ matrix directions. This is in agreement with the observations of Kim and Park [24] in the case of a high copper AlLiCuMgZr alloy in the unstretched condition. The mean size of T_1 precipitates for A, B and C alloys in the peak-aged condition is 190, 185 and 165 nm respectively. This reduction of the size of T_1 precipitates is marginal, if one considers that the experimental error is quite large, i.e. $\pm$ 15 nm as a consequence of the small number of the T_1 precipitates measured. Nevertheless, it may suggest a trend of reducing the size of T_1 precipitates as the Ag content of the alloys is increased. The same argument, as in the

case of δ′ precipitates, can be used to explain this tendency, i.e., as the Ag concentration increases, the solubility of Li in the matrix rises and consequently the number of available Li atoms for the growth of T_1 precipitates diminishes.

The above observations generally agree with the calculated diagrams of phase transformations on ageing by Alekseev *et al.* [25]. They estimate that the major phases present in AlLiCuMg alloys with a composition equivalent to that of A, B and C alloys (without Ag) and for the ageing conditions adopted, would be δ′, S' and T_1.

Minor additions of Ag in AlCuMg alloys result in the precipitation of Ω phase especially in alloys with a high Cu : Mg ratio [7–9, 26–29]. The structure of this phase has been a subject of discussion [7–9, 27]. The most likely structure seems to be that proposed by Knowles and Stobbs [8], i.e., orthorhombic with $a = 0.496$ nm, $b = 0.859$ nm and $c = 0.848$ nm. The Ω phase grows as thin plate-shape precipitates on $\{1\,1\,1\}$ matrix planes. The distinction of Ω and T_1 precipitates is not trivial for the following reasons [6, 8, 28]: (a) Their habit planes are the same, i.e., $\{1\,1\,1\}$ matrix planes, (b) they both grow as thin plates and (c) the selected area diffraction patterns obtained cannot be distinguished due to almost identical allowable reflections and excessive streaking. Therefore, assuming the structure proposed by Knowles and Stobbs, the X-ray diffraction pattern of the Ω phase was calculated using the Rietveld method [30, 31]. It was not possible to fit the experimental X-ray diffraction spectrums of B and C alloys to the calculated one. This suggests that the Ω phase is not precipitating in these alloys. The Cu : Mg ratio in these alloys is ~ 1.8 whilst Ω precipitates have been observed in alloys with a ratio higher than 5 [e.g., 6, 9]. Consequently it is concluded that alloys B and C do not lie in the appropriate phase field for the precipitation of the Ω phase.

On the contrary the Cu : Mg ratio in alloy D is 5. The experimental X-ray diffraction pattern of this alloy, in both under- and peak-aged conditions could be fitted to the Rietveld simulated spectrum. In Fig. 8 the experimental XRD spectrum of alloy D in the under-aged condition is presented. The arrows correspond to the positions of the Ω fitted peaks. Consequently it may be concluded that the Ω phase precipitates in alloy D, provided that the Ω phase structure used is correct. TEM examination of this alloy revealed a quite different microstructure compared with alloys A, B and C. Fig. 9a is a typical bright field micrograph whilst Fig. 9b is the associated selected area diffraction pattern indicating that the foil normal is $[\bar{1}\,1\,2]$. A rather homogeneous distribution of edge-on $\{111\}$ plate like precipitates (Ω/T_1) can be seen. Inclined precipitates of hexagonal shape can also be noticed. Ω precipitates usually obtain such a hexagonal shape for symmetry reasons [7, 26]. The volume fraction of Ω/T_1 precipitates is much higher in alloy D than in alloys B and C. In the same micrograph S' laths are also observed. The volume fraction of S' precipitates is comparable to that of $\{111\}$ precipitates in this alloy.

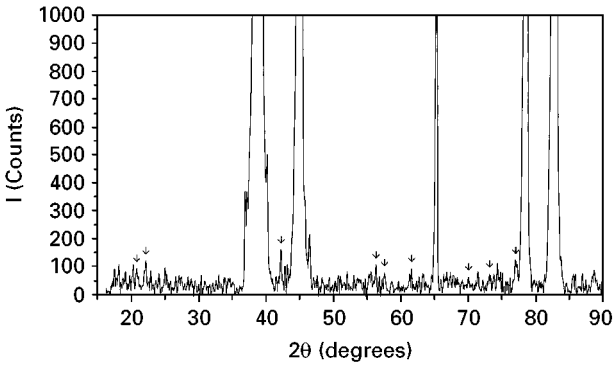

Figure 8 XRD spectrum of D alloy. The arrows indicate Ω phase peaks.

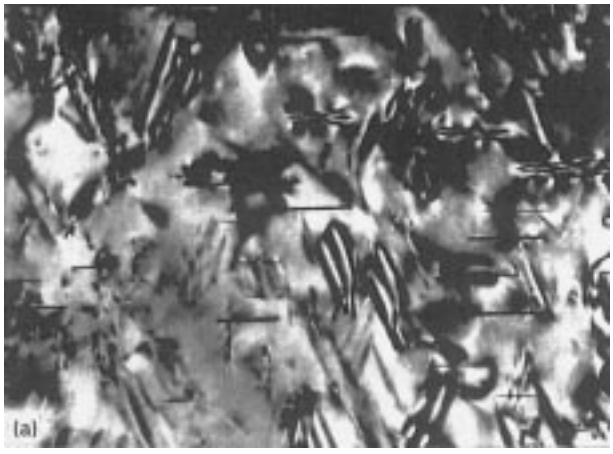

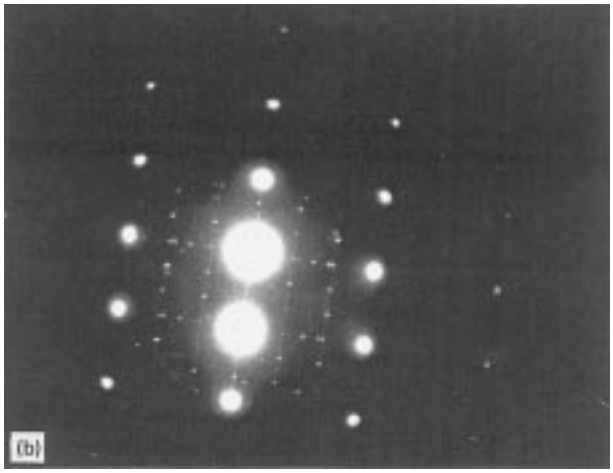

Figure 9(a) BF micrograph of edge-on Ω/T_1 of peak-aged D alloy. Magnification × 88 000; (b) associated SAD pattern indicating $[\bar{1}\,1\,2]$ zone axis.

Another significant microstructural feature is an unusual precipitation of the δ′ phase. As can be seen in Fig. 10 the plain δ′ precipitates in the under-aged alloy are quite small (mean diameter 18 nm), whilst the composite δ′/β′ ones are very big (mean diameter 90 nm). The "coffee-bean" contrast of the δ′ precipitates is due to a strain field effect [32]. Also the distribution of δ′ precipitates is not as homogeneous as that observed in alloys A, B and C and their volume fraction is somewhat lower as well. This can be explained as follows. The Li concentration in alloy D is 1.5 wt % while in alloys A, B and C it is 2.4 wt %. This

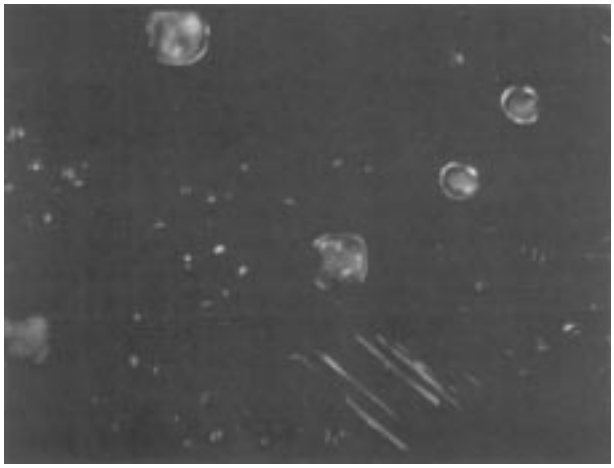

Figure 10 DF micrograph of δ′ and δ′/β′ precipitates of under-aged D alloy. Magnification × 88 000.

reduction of Li results in a decrease of (a) the volume fraction and (b) of the size of δ′ precipitates below a critical size that gives rise to their dissolution during ageing. The Li atoms thus provided, contribute to the subsequent growth of the originally larger and more stable δ′/β′ composite precipitates. So as the ageing time increases the δ′/β′ precipitates grow at the expense of the δ′ ones. In the peak aged condition the δ′ superlattice spots were detected, as can be seen in Fig. 9b, verifying the existence of δ′ phase. Since these spots were very weak we could not obtain a dark field micrograph of the δ′ precipitates.

4. Conclusions

Four Al–Li–Cu–Mg based alloys have been studied by means of transmission electron microscopy, X-ray diffraction and optical microscopy. In the high Li, low Cu : Mg ratio alloys the main phases found are δ′, β′, S' and T_1, while fewer T_2 and Al_7Cu_2Fe precipitates were also observed. The volume fraction of S' precipitates is much higher than that of T_1 ones, while their morphology is mainly rod-like. The addition of Ag up to 0.5 wt % slightly reduces the size of the δ′ and T_1 precipitates and consequently seems to result in a small increase of the Li solubility in the matrix but otherwise did not have any major influence on the microstructure of these alloys. On the contrary the addition of 0.2 wt % Ag in the low Li, high Cu : Mg ratio alloy resulted in a concurrent precipitation of Ω phase. The volume fraction of Ω/T_1 precipitates was comparable with that of S' precipitates. An unusual growth and size distribution of the plain δ′ and of the composite δ′/β′ precipitates has been also observed and attributed to the dissolution of the former in favour of the later.

Acknowledgements

The present study has been carried out under the Brite-Euram project "SALLI" Contract No. BRE2-T92-0250. The authors are grateful to Dr. D. McDarmaid of Defence Research Agency for supplying the alloys and Dr. A. Smith of Westland Helicopters Ltd for allowing the publication of the present study.

References

1. T. H. SANDERS Jr and E. A. STARKE Jr, in Proceedings of Aluminium–Lithium Alloys II, edited by T. H. Sanders Jr and E. A. Starke Jr (AIME, Warrendale, PA, USA, 1983) p. 1.
2. E. LAVERNIA and N. GRANT, *J. Mater. Sci.* **22** (1987) 1521.
3. D. B. WILLIAMS and J. W. EDINGTON, *Metall. Sci. J.* **9** (1975) 529.
4. T. H. SANDERS Jr and E. A. STARKE Jr, in Proceedings of Advanced Aluminium and Magnesium Alloys, edited by T. Khan and G. Effenberg (ASM, Amsterdam, Holland, 1990) p. 13.
5. P. SAINFORT and B. DUBOST, in Proceedings of the 4th International Aluminium–Lithium Conference edited by G. Champier, B. Dubost, D. Miannay and L. Sabetay, *J. Phys. Colloque* **C3** (1987) 407.
6. R. HERRING, F. GAYLE and J. PICKENS, *J. Mater. Sci.* **28** (1993) 69.
7. B. MUDDLE and J. POLMEAR, *Acta Metall.* **37** (1989) 777.
8. K. KNOWLES and W. STOBBS, *Acta Cryst.* **B44** (1988) 207.
9. S. ABIS, P. MENGUCCI and G. RIONTINO, *Phil. Mag. B* **67** (1993) 465.
10. A. SMITH, Private communication.
11. P. KELLY, A. JOSTSONS, R. BLAKE and J. NAPIER, *Phys. Stat. Sol.* **A31** (1975) 771.
12. G. GU, G. LIEDL, T. SANDERS Jr and K. WELPMANN, *Mat. Sci. Engng.* **76** (1985) 147.
13. F. GAYLE and J. VANDER SANDE, *Scr. Metall.* **18** (1984) 473.
14. E. A. STARKE Jr, T. H. SANDERS Jr and I. G. PALMER, *J. of Metals* **33** (1981) 24.
15. S. BAUMANN and D. WILLIAMS, in Proceedings of Aluminium–Lithium Alloys II, edited by T. H. Sanders Jr and E. A. Starke Jr (AIME, Warrendale, PA, USA, 1983) p. 17.
16. C. BARTGES, M. TOSTEN, P. HOWELL and E. RYBA, *J. Mater. Sci.* **22** (1987) 1663.
17. M. AUDIER and P. GUYOT, *Phil. Mag. Lett.* **58** (1988) 17.
18. W. CASSADA, G. SHIFLET and S. POON, *Phys. Rev. Lett.* **56** (1986) 2276.
19. A. GUPTA, P. GUANT and M. CHATURVEDI, *Phil. Mag. A* **55** (1987) 375.
20. C. ZHANG, W. SUN and H. YE, *Phil. Mag. Lett.* **59** (1989) 265.
21. V. RADMILOVIC, G. THOMAS, G. SHIFLET and E. A. STARKE Jr, *Scripta. Metall.* **23** (1989) 1141.
22. B. NOBLE and G. THOMPSON, *Metall. Sci. J* **6** (1972) 167.
23. J. HUANG and A. ARDELL, *Mater. Sci. and Tech.* **3** (1987) 176.
24. J. KIM and J. PARK, *Metall. Trans. A* **24A** (1993) 2613.
25. A. ALEKSEEV, V. ANAN'EV, L. BER and A. SHESTAKOV, *Phys. Met. Metallograph.* **77** (1994) 415.
26. A. GARG and J. HOWE, *Acta Metall. Mater.* **39** (1991) 1925.
27. *Idem*, *ibid.* **39** (1991) 1939.
28. T. LANGAN and J. PICKENS, in Proceedings of the 5th International Aluminium–Lithium Conference edited by T. H. Sanders Jr and E. A. Starke Jr (MCE, Birmingham, UK, 1989) p. 691.
29. R. FONDA, W. CASSADA and G. SHIFLET, *Acta Metall. Mater.* **40** (1992) 2539.
30. H. RIETVELD, *J. Appl. Cryst.* **2** (1969) 65.
31. R. YOUNG and D. WILES, *ibid.* **15** (1980) 430.
32. J. EDINGTON, in "Practical Electron Microscopy in Materials Science" (MacMillan Press Ltd, 1974).

Received 10 August 1995
and accepted 13 February 1996